

Pilot Model Development and Human Manual Control Considerations for Helicopter Hover Displays

Friesen, Daniel; Pavel, Marilena; Borst, Clark; Masarati, Pierangelo; Mulder, Max

Publication date

2019

Document Version

Final published version

Published in

45th European Rotorcraft Forum 2019, ERF 2019

Citation (APA)

Friesen, D., Pavel, M., Borst, C., Masarati, P., & Mulder, M. (2019). Pilot Model Development and Human Manual Control Considerations for Helicopter Hover Displays. In *45th European Rotorcraft Forum 2019, ERF 2019* (pp. 565-578). Article Paper 33 (45th European Rotorcraft Forum 2019, ERF 2019; Vol. 1).

Important note

To cite this publication, please use the final published version (if applicable).
Please check the document version above.

Copyright

Other than for strictly personal use, it is not permitted to download, forward or distribute the text or part of it, without the consent of the author(s) and/or copyright holder(s), unless the work is under an open content license such as Creative Commons.

Takedown policy

Please contact us and provide details if you believe this document breaches copyrights.
We will remove access to the work immediately and investigate your claim.

PILOT MODEL DEVELOPMENT AND HUMAN MANUAL CONTROL CONSIDERATIONS FOR HELICOPTER HOVER DISPLAYS

Daniel Friesen^{1,2}, Marilena D. Pavel¹, Clark Borst¹, Pierangelo Masarati², and Max Mulder¹

¹Delft University of Technology (Kluyverweg 1, 2629 HS Delft, The Netherlands)
{d.friesen, m.d.pavel, c.borst, m.mulder}@tudelft.nl

²Politecnico di Milano (Via La Masa 34, 20156 Milano, Italy)
{daniel.friesen, pierangelo.masarati}@polimi.it

Abstract

Head-down hover displays and instrument panels theoretically provide all necessary flight data information to control low-speed helicopter manoeuvring. However, past experiments have shown that head-down displays can incur high workload, control instability, and even loss of control when used as the sole flight data source. This paper investigates the reasons for this instability incurred by replacing good outside visuals with a head-down hover display and an instrument panel. A pilot model based on crossover theory is developed for a linear six-degree-of-freedom Bo105 helicopter model. Utilising a target trajectory based on τ -theory and assuming perfect information availability, the developed model can perform the required manoeuvring task with a control time-delay stability margin of 0.15 s (with SAS) or 0.17 s (without SAS). Then, the actual information availability based on human perception methods and limitations is discussed. A pilot-in-the-loop experiment in the SIMONA Research Simulator qualitatively validates the developed pilot model for good outside visuals. However, the pilot model does not capture the added difficulties of having to utilise the hover display and instrument panel instead of good outside visuals; during the experiment, the task was impossible to complete with only these displays. This is likely caused by an increase in control time-delay, which in turn is caused by the loss of peripheral and flow field information, a more abstract information representation compared to good outside visuals, and the fact that the pilot now needs to scan multiple displays to acquire all necessary flight state information. Improving head-down hover display symbology and scaling factors might rectify some, but probably not all of these effects.

NOMENCLATURE

\mathbf{a}_{hor} [m/s ²]	Helicopter horizontal acceleration vector	\mathbf{x}	Vector of state space system states
\mathbf{c}_{acc} [m]	Hover display horizontal acceleration cue vector	ω [rad/s]	Frequency
\mathbf{c}_{vel} [m]	Hover display horizontal velocity cue vector	ω_c [rad/s]	Crossover frequency
\mathbf{u}	Vector of state space control inputs	ω_i [rad/s]	Forcing function bandwidth
\mathbf{v}_{hor} [m/s]	Helicopter horizontal velocity vector	ϕ [rad]	Euler roll angle
		[rad]	Euler yaw angle
		τ_e [s]	Effective time-delay
		θ [rad]	Euler pitch angle
		θ_0 [rad]	Collective input
		θ_{1c} [rad]	Lateral cyclic input
		θ_{1s} [rad]	Longitudinal cyclic input
		θ_{TR} [rad]	Pedal/tail rotor collective input
		φ_m [rad]	Phase margin
		A	State space model matrix
		A_{SAS}	State space model matrix with SAS

Copyright Statement

The authors confirm that they, and/or their company or organization, hold copyright on all of the original material included in this paper. The authors also confirm that they have obtained permission, from the copyright holder of any third party material included in this paper, to publish it as part of their paper. The authors confirm that they give permission, or have obtained permission from the copyright holder of this paper, for the publication and distribution of this paper as part of the ERF proceedings or as individual offprints from the proceedings and for inclusion in a freely accessible web-based repository.

B	State space control matrix
F	Matrix of SAS parameters
K_m [-]	Gain margin
K_p [-]	Pilot gain
p [rad/s]	Body roll rate
q [rad/s]	Body pitch rate
r [rad/s]	Body yaw rate
T_I [s]	Lag time constant
T_L [s]	Lead time constant
T_{acc} [s]	Hover display acceleration scaling factor
T_{vel} [s]	Hover display velocity scaling factor
u [m/s]	Body surge velocity
v [m/s]	Body sway velocity
w [m/s]	Body heave velocity
x [m]	Body longitudinal position
y [m]	Body lateral position
Y_c	Controlled element transfer function
Y_p	Pilot model transfer function
Y_{CL}	Closed-loop transfer function
Y_{OL}	Open-loop transfer function
z [m]	Body vertical position

ACRONYMS

ADS-33	Aeronautical Design Standard 33E-PRF
Bo105	Messerschmitt-Bölkow-Blohm Bo105 Helicopter
DVE	Degraded Visual Environment
HDD	Head-Down Display
HMD	Helmet-Mounted Display
HUD	Head-Up Display
NITROS	Network for Innovative Training on Rotorcraft Safety
SAS	Stability Augmentation System
SRS	SIMONA Research Simulator
UCE	Usable Cue Environment
V/STOL	Vertical and/or Short Take-Off and Landing

1. INTRODUCTION

When a helicopter enters a Degraded Visual Environment (DVE), the amount of visual cues that is available to the pilot decreases — the Usable Cue Environment (UCE)-level increases from level 1, which represents near perfect visibility, to level 2 or 3. A DVE can be caused by, e.g., a brown-out/white-out, nightfall or dense fog. In order to maintain good operability of helicopters under worsening visibility conditions, different Head-Up Display (HUD) and Head-Down Display (HDD) systems can be employed. These displays can decrease the UCE-level by providing the pilot with additional flight state data and information about the attitude and position of the helicopter with respect to its environment. While many different display systems are possible (see Minor et al.¹ for an overview and Münsterer et al.² or Stanton et al.³ for current HUD examples), this paper focuses on the analysis of two-dimensional hover displays.

In this paper, hover displays are defined as visualisations of the horizontal position of the helicopter with respect to objects or locations in the environment, for example, hover target points or landing zones. In many existing displays, additional information about the horizontal velocity and acceleration is shown. The information is represented in a top-down view, with the helicopter at its centre. Information about the yaw angle is apparent through the rotation of the environmental objects around the centre of the display. Altitude information is not inherently part of a hover display, but often represented in close vicinity in the cockpit through an altimeter or an altitude tape.

Many concepts of two-dimensional hover displays have been described in literature — either as a separate HDD, or as a two-dimensional projection on top of a (synthetic) three-dimensional outside view (HDD or HUD), for example by Hess and Gorder⁴, Eshow and Schroeder⁵, or Szobozlay et al.⁶. A comparison of different Vertical and/or Short Take-Off and Landing (V/STOL) displays for approach and landing, hover displays among them, has already been conducted in the year 1972⁷. However, according to a literature review and flight experiments described by Minor et al., panel-mounted HDD are not suitable as the source of primary flight data for the pilot: "flight using only a scaled panel mounted image, even at 20/20 day visual acuity, is uncontrollable at low airspeeds in most rotorcraft (...) during high-gain tasks such as approach and landing"¹.

While hover displays theoretically provide all necessary aircraft attitude and position information that is required to maintain a controlled flight, they

seem to incur additional problems that prohibit pilots from using them as the sole flight data information source. This paper investigates possible reasons for these added complexities by employing a control-theoretic approach: it investigates the replacement of good outside visuals with a head-down hover display and instrument panel during a helicopter hovering task, with and without an activated Stability Augmentation System (SAS). Simulated pilot model data and experimental pilot-in-the-loop data are compared and analysed to identify and quantify the reasons why hover displays appear to be unsuited for being the sole source of flight data information for the pilot.

The goal of the paper is threefold:

1. analyse the requirements placed on the pilot control models by low speed helicopter flight with and without a SAS, and identify stability margins ("controllability analysis");
2. analyse the requirements placed on the pilot's visual perceptual system by (1) good outside visuals and (2) zero visuals with a hover display and instrument panel, to acquire the necessary system state information and provide the state input for the previously described control loops ("observability analysis");
3. combine these analyses to identify possible causes for closed loop control instability when switching from good outside visibility to a hover display and instrument panel, and formulate design strategies and requirements to minimise these effects.

Section 2 highlights background information about the utilised helicopter model, hover display and pilot model. The following sections 3 and 4 contain the controllability analysis and observability analysis, respectively. The performance of the developed pilot model is compared with data collected during a pilot-in-the-loop experiment in Section 5. Section 6 discusses the results of the previous analyses and experiment, identifying possible causes for instability and formulating display design recommendations. Conclusions are presented in Section 7.

2. BACKGROUND

In this section, the utilised helicopter model, its modifications, and the employed hover display are introduced. Lastly, this section describes the human control model based on crossover theory and its applicability to this paper's control task.

2.1. Helicopter model

A linear six degree of freedom state-space model of a Messerschmitt-Bölkow-Blohm Bo105 Helicopter (Bo105) trimmed at zero forward flight speed is used as the simulation test bed. The model matrix A and control matrix B have been adapted from Padfield⁸ to also include position and yaw-angle information. The order of states is rearranged to cluster the states of the surge (4), heave (2), sway (4) and yaw (2) motion. This results in the state vector

$$(1) \quad \mathbf{x} = (x, u, \theta, q, z, w, y, v, \phi, p, \psi, r)$$

and the control vector

$$(2) \quad \mathbf{u} = (\theta_{1s}, \theta_0, \theta_{1c}, \theta_{TR})$$

of the dynamic system

$$(3) \quad \dot{\mathbf{x}} = A\mathbf{x} + B\mathbf{u}$$

2.2. SAS implementation

A SAS is incorporated directly into system matrix A_{SAS} according to equation 4 by assuming zero time-delay, zero noise and unity transfer functions for SAS sensors and actuators. The Bo105 SAS parameters in matrix F are based on previous tuning experiments conducted at TU Delft as part of the ARISTOTEL project*.

$$(4) \quad A_{SAS} = A + BF$$

The effect of the SAS can be observed in the complex plane representation of the system's poles in Figure 1, as well as in Bode plots of the simplified inner loop controlled element transfer functions $Y_{c,inner}$ in Figure 8 (Section 3 details how the transfer functions are determined). Two pairs of complex poles with non-zero imaginary parts are converted into four poles with only negative real parts, and the amplitude peaks of the controlled element transfer functions in the surge and sway loops are reduced. While the SAS damps some elements of the system, the unstable phugoid mode (represented by a pair of complex poles with positive real parts) is still evident.

*No published documents pertaining to ARISTOTEL SAS parameters publicly available. General information at <http://aristotel-project.eu/welcome/>

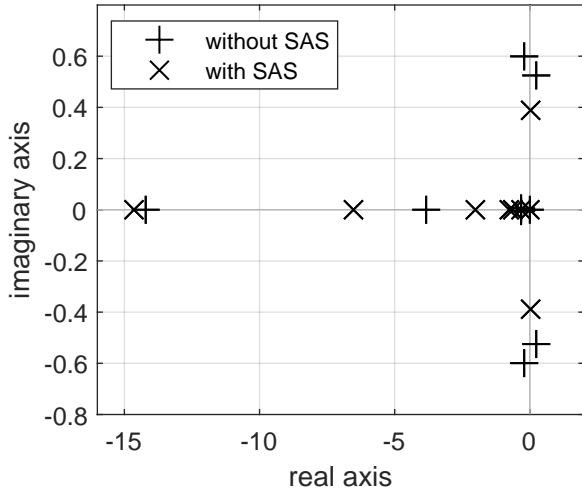


Figure 1: Poles of the system matrix A with and without SAS.

2.3. Hover display

As explained in the introduction, a hover display and instrument panel can supply the pilot with all necessary attitude and altitude information to control the helicopter in case of DVE conditions. When the UCE-level increases, hover displays provide means to perceive the necessary information through an abstracted top-down view.

Figure 2 depicts the hover display used and analysed in this paper. It is based on the "baseline" hover display explained by Hess and Gorder⁴, incorporating a generalisation of the scaling factors to allow separate scaling for the velocity and acceleration cues. The display is scaled such that it shows the ground in a 80 m diameter. The hover target area represents the desired position, and the ground reference markings mark the desired approach path from the starting position to the hover target position. The display rotates such that the heading of the helicopter always points upwards.

The horizontal velocity cue \mathbf{c}_{vel} is a straight line representing the direction and magnitude of the current horizontal velocity, with its origin at the centre of the current helicopter position. It is scaled with respect to actual distance in the physical world:

$$(5) \quad \mathbf{c}_{vel} = T_{vel} \mathbf{v}_{hor}$$

The scaling factor is chosen to be $T_{vel} = 3\text{ s}$, which is then multiplied with the horizontal velocity of the helicopter \mathbf{v}_{hor} . The velocity cue represents a linear prediction of horizontal position with a look-ahead time of T_{vel} . As an example, a horizontal velocity of $10 \frac{\text{m}}{\text{s}}$ creates a cue of 30 m, which is then

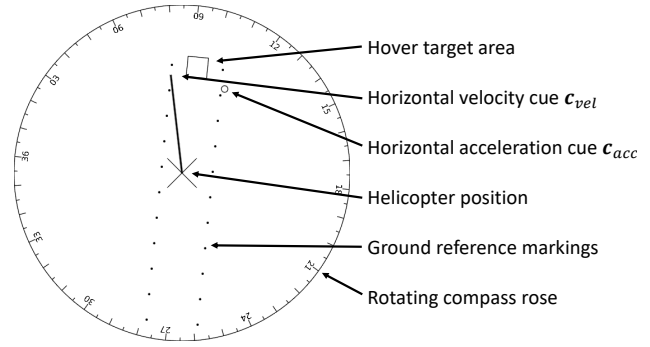


Figure 2: Hover display elements.

translated to the display via the display scaling factor of 80 m per diameter. The value of T_{vel} is chosen such that at the beginning of the experimental scenario, the velocity cue fills 75 % of the available display space between the centre and the edge, enabling the use of the majority of the available display space during the deceleration manoeuvre.

The acceleration cue \mathbf{c}_{acc} is calculated via:

$$(6) \quad \begin{aligned} \mathbf{c}_{acc} &= \mathbf{c}_{vel} + T_{acc} \dot{\mathbf{c}}_{vel} \\ &= T_{vel} \mathbf{v}_{hor} + T_{vel} T_{acc} \mathbf{a}_{hor}, \end{aligned}$$

with the horizontal acceleration of the helicopter \mathbf{a}_{hor} and the acceleration scaling factor $T_{acc} = 1.5\text{ s}$. Selecting $T_{acc} = 0.5 \cdot T_{vel}$ and defining the tip of the velocity cue as origin for the acceleration cue (already incorporated in Equation 6) leads to the acceleration cue representing a quadratic prediction of horizontal position, again with a look-ahead time of T_{vel} . These values are chosen in order to generate consistency between the cues: the velocity-cue \mathbf{c}_{vel} represents the linear prediction, the acceleration-cue \mathbf{c}_{acc} represents the quadratic prediction of horizontal position, both with a look-ahead time of $T_{vel} = 2 \cdot T_{acc} = 3\text{ s}$.

2.4. Crossover model

The crossover model as described by McRuer and Jex⁹ enables the development of models of human control for a variety of dynamic systems. The transfer function of the human controller is given by:

$$(7) \quad Y_p(s) = K_p \frac{1 + T_L s}{1 + T_I s} \cdot e^{-\tau_e s},$$

with gain K_p , lead- and lag-constants T_L and T_I , and the lumped time-delay τ_e . The crossover model postulates how human controllers modify the lead- and lag-constants of their control behaviour to maximise task performance and maintain stability.

Several pilot models of this form are developed in this paper to control the various degrees of freedom of the described helicopter model. It is important to note that McRuer and Jex only validated this model for single-axis disturbance-rejection tasks with a compensatory display, while the approach-to-hover task described in this paper is a coupled multi-axis stabilisation task, with a pursuit display that includes some preview display characteristics. Nonetheless, tuning and analysing these model parameters give some insight into the peculiarities of this control task.

3. CONTROLLABILITY ANALYSIS

In this section, a basic control analysis of six-degree-of-freedom helicopter hovering flight dynamics is conducted. Required control loops and pilot model architectures are discussed. Basic pilot models based on the crossover model⁹ are developed and tuned for flight with and without a SAS. They are combined with target trajectories based on τ -theory¹⁰ to generate sample approach-to-hover manoeuvres. Critical control loops and control theoretic bottlenecks to maintain stability are identified and discussed.

3.1. System simplification

The system matrix is simplified and most cross-couplings are neglected to enable the development and tuning of basic pilot models based on the crossover model for each control loop. The system is decoupled into four separate dynamic systems: longitudinal position/surge control, height/heave control, lateral position/sway control, and yaw angle/yaw rate control.

As an example, the structure of the longitudinal position control loop in hover is depicted in Figure 3, with longitudinal position x , longitudinal velocity u , body pitch angle θ and longitudinal cyclic control θ_{1s} . The controlled parameter chain is therefore $(\theta_{1s} \rightarrow \theta \rightarrow u \rightarrow x)$. A subscript t denotes control target values, a subscript e denotes control error values, a parameter without subscript denotes the actual system state. System structures to control heave ($\theta_0 \rightarrow w \rightarrow z$), sway ($\theta_{1c} \rightarrow \phi \rightarrow v \rightarrow y$) and yaw ($\theta_{TR} \rightarrow r \rightarrow \psi$) are set up similarly.

The transfer functions from the control input to the first considered inner loop system state (θ for surge, w for heave, ϕ for sway, r for yaw) are calculated with all remaining coupling coefficients within the four decoupled systems. However, The following middle loop states (u for surge, z for heave, v for sway, ψ for yaw) and outer loop states (x for surge, y for sway) are furthermore assumed to only

depend on the previous system state in the chain. Cross-control effects and couplings between states in the same chain are neglected.

3.2. Pilot model development

McRuer and Jex's verbal adjustment rules⁹ are used to develop models of human controllers for each of the four cascading control loops. Stability and phase margin techniques in the frequency domain are used to tune the pilot model gains, in order to achieve good performance and stability.

The first step in developing the inner loop pilot models is to determine the required lead- and lag-constants T_L and T_I to create an open loop amplitude slope of -20 dB/decade in the area of the crossover frequency. The crossover frequency ω_c is assumed to be around $\omega_c \approx (1 - 5) \frac{\text{rad}}{\text{s}}$. The effective time-delay is approximated as $\tau_e = 0.295$ s, calculated with a hypothetical forcing function bandwidth of $\omega_i = 1 \frac{\text{rad}}{\text{s}}$. (This task does not contain a forcing function, ω_i has been chosen as an arbitrary and small value.)

After determining T_I , T_L , and τ_e , the pilot gain K_p is tuned by choosing the maximum value for K_p for which the open loop transfer function Y_{OL} still has a phase margin $\varphi_m \geq 60^\circ$ and a gain margin $K_m \geq 3$. Middle and outer loop controllers consist of only a gain, without lead-,lag- or time-delay-parameters. The crossover frequency is required to be at most half the crossover frequency of the previous loop.

3.3. Example: surge pilot model tuning

As an example, the tuning process of the unaugmented surge control loops is described here, starting with the **inner loop**. The inner loop controlled element transfer function $Y_{c,inner}$ is depicted in Figure 8. It has is an amplitude peak at $\omega = 0.52 \frac{\text{rad}}{\text{s}}$, caused by two complex poles at $(0.0341 \pm 0.5153i)s^{-1}$, representing the phugoid motion. A third pole is located on the real axis at $-3.8365s^{-1}$, causing a slope decrease from -20 dB/decade to -40 dB/decade at $\omega = 3.8365 \frac{\text{rad}}{\text{s}}$. To create a slope of -20 dB/decade in the area of the crossover frequency, the pilot model parameter T_L is set to the inverse of the highest frequency pole: $T_L = 0.2607$ s. Afterwards, the gain K_p is tuned such that the phase margin and gain margin criteria are met. The resulting inner loop pilot model transfer function $Y_{p,inner}$ is depicted in Figure 9, the inner loop open loop transfer function $Y_{OL,inner}$ in Figure 10.

The **middle loop** equivalent controlled element transfer function $Y_{c,middle,equivalent}$ is computed by multiplying the inner loop closed loop transfer function $Y_{CL,inner}$ with the middle loop controlled el-

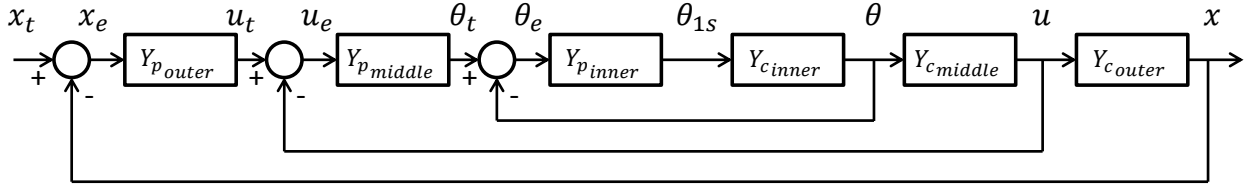


Figure 3: Structure of the controlled augmented horizontal longitudinal system.

element dynamics $Y_{c,middle}$. The middle loop pilot model $Y_{p,middle}$, represented by only a gain, is now tuned such that the middle loop open loop transfer function $Y_{OL,middle}$ satisfies the crossover frequency, phase margin and gain margin criteria.

Similarly, the **outer loop** equivalent controlled element transfer function $Y_{c,outer,equivalent}$ is computed by multiplying the middle loop closed loop transfer function $Y_{CL,middle}$ with the outer loop controlled element dynamics $Y_{c,outer}$. The outer loop pilot model $Y_{p,outer}$ is tuned such that the outer loop open loop transfer function $Y_{OL,outer}$ satisfies the tuning constraints, leading to the outer loop closed loop transfer function $Y_{CL,outer}$.

3.4. Tuned pilot model

Table 1 shows crossover frequencies, phase-, and gain-margins of every controlled loop, Figures 11 and 12 show Bode plots of the closed loop transfer functions without and with SAS. The phase margin criterion is critical in two cases (unaugmented inner loops of surge and sway). In the other cases, the gain-margin is the inner loop's critical tuning parameter, followed by either the frequency criterion or another gain-margin criterion in the next loops.

The tuned pilot model was evaluated while controlling the fully coupled system. Control time-delay stability margins are shown in table 2. While the margins are reduced for every degree of freedom when switching the SAS off, the combined tolerable time-delay is slightly higher without a SAS. This might be caused by the generally lower pilot gains in the no-SAS configuration, and a consequential reduction of the intensity of cross-coupling effects.

The development of the pilot models with only the simplified decoupled system represents a limitation on their applicability on the fully coupled system. Nevertheless, the pilot models have been successfully applied to the fully coupled state space system, with reasonable performance and stability close to hover. The coupled controlled system is able to perform low-speed position-following manoeuvres, utilising a three dimensional target position and a target yaw angle as reference. Figure 4

shows the system response to a generic target trajectory.

It is important to note that a pilot model based on the crossover model "(...) should not be used, without appropriate modification, to compute the system response to a deterministic input such as a step.", as McRuer and Jex noted⁹. The pilot models in this paper are not modified in any way before their time response is computed. The presented results can therefore only serve as qualitative comparison data; a rigid, quantitative analysis in the time-domain is not feasible.

4. OBSERVABILITY ANALYSIS

The previous section assumes perfect information availability for the pilot. In this section, the requirements resulting from the control theoretic analysis are compared with the actual nature of information supply provided by (1) good outside visuals and (2) a hover display. Good outside visuals assume a helicopter position reasonably close to the ground, such that texture and existing objects supply the pilot with all necessary optical cues (Usable Cue Environment (UCE)-level 1). A basic flight instrument panel and hover display, developed at TU Delft, serves as analysis test bed (Figure 5).

The following subsection elaborates on the characteristics of the analysed display system. Then, modes of perception for different system states are shown, and typical perceptual and control time-delays of human controllers are discussed.

4.1. Display implementation

The utilised hover display is described in Subsection 2.3. For this analysis, the display's size and location in the SRS is used. It is shown on a monitor at a distance of 90 cm to the pilot's eyes, its centre approximately 10° inclined downwards from the horizon and approximately 20° to the left. The hover display diameter is 18 cm, which translates to 10.3° in the pilot's visual field. 1 cm of display relates to 0.57° of visual separation.

Table 1: Crossover frequencies, gain- and phase-margins of every controlled loop. *critical tuning parameter

System	Loop	Target	without SAS			with SAS		
			ω_c [rad/s]	K_m [-]	φ_m [deg]	ω_c [rad/s]	K_m [-]	φ_m [deg]
Surge	Inner	θ	1,61	3,62	*60,1	1,74	*3,00	95,9
	Middle	u	*0,80	3,58	70,9	*0,87	3,40	72,2
	Outer	x	0,38	*3,03	66,0	*0,43	4,47	62,4
Heave	Inner	w	1,81	*3,01	69,4	1,81	*3,01	69,4
	Middle	z	*0,90	3,11	63,5	*0,90	3,11	63,5
Sway	Inner	ϕ	1,73	3,35	*60,1	1,91	*3,01	61,4
	Middle	v	*0,86	3,29	70,2	0,93	*3,01	69,4
	Outer	y	0,41	*3,00	64,6	*0,46	3,10	62,9
Yaw	Inner	r	1,81	*3,01	69,3	1,78	*3,02	63,2
	Middle	ψ	*0,91	3,09	63,3	*0,89	3,10	61,8

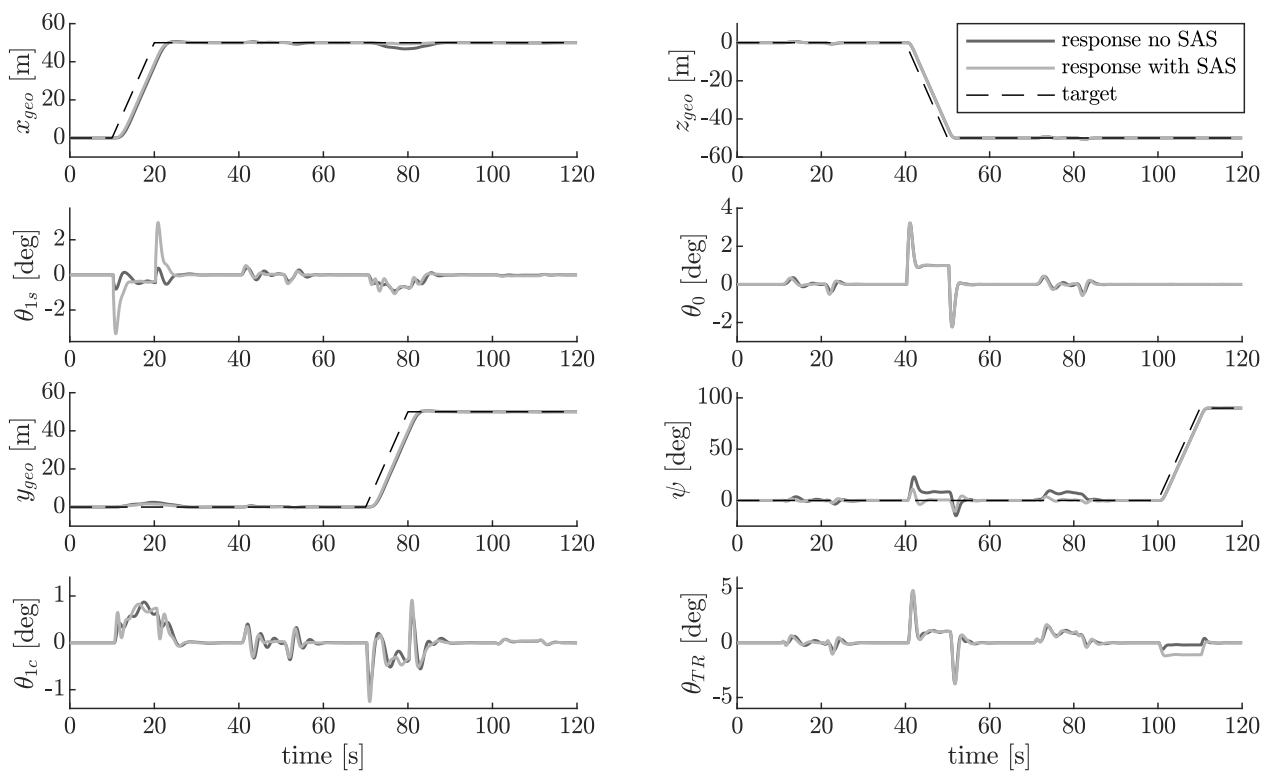


Figure 4: Pilot model response with the coupled system to sequential ramp targets in every loop.

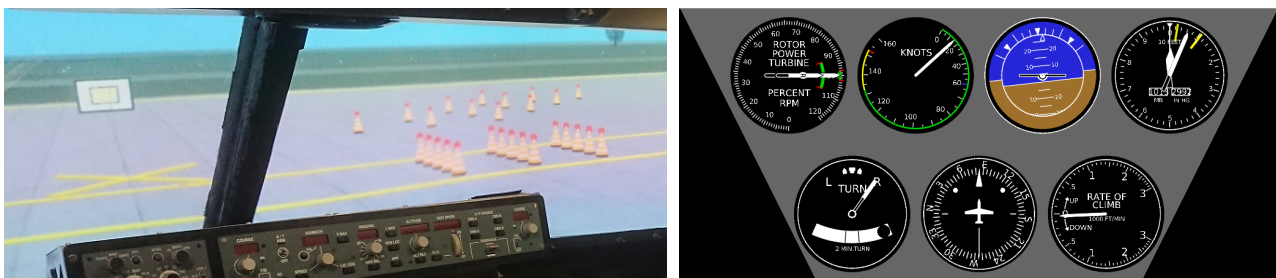


Figure 5: Outside scenery while approaching the hover target area (left) and primary flight display (right).

Table 2: Inner loop time-delay stability margins of the coupled system. "Combined" denotes a time-delay introduced in every inner loop at the same time.

time-delay margin [s]	With SAS	Without SAS
Surge	0.34	0.28
Heave	0.42	0.37
Sway	0.26	0.25
Yaw	0.34	0.28
Combined	0.15	0.17

4.2. Human perception

Table 3 contains a broad categorisation of pilot perception methods for all necessary system states. While the outside view provides means to perceive every required system state, the instrument panel and the hover display are lacking specific information about x , v , y , or w , z , respectively. Controlling the helicopter without outside visuals requires the integration of information from both displays.

4.3. Time-delay

Hosman and Stassen¹¹ performed an experiment to determine the necessary visual exposure time that is required for a pilot to generate an adequate control response to a roll attitude stimulus. They also measured the reaction time between the start of exposure and the onset of the control action. The lumped perception-action time-delay of their pilot model controlling a double-integrator system is set to $\tau_I = 0.2$ s. Similarly, Drop¹² applies a lumped pilot model delay of 0.3 s to control helicopter longitudinal motion.

Time-delays of this magnitude have been identified by McRuer and Jex⁹ for double integrator system dynamics. They were identified based on single input, single output disturbance rejection tasks for double integrator system dynamics. Controlling a helicopter requires the simultaneous control of four system states. Increasing the number of loops controlled in parallel decreases performance and increases the effective time-delay of the controller¹³. The utilised time-delay of $\tau_e = 0.295$ s in this paper seems to be reasonably close to comparable values from single- or double-axis control tasks in literature.

5. PILOT-IN-THE-LOOP EXPERIMENT

After Section 3 establishes the pilot model parameters, and Section 4 confirms the magnitude of time-delay and the theoretic possibility of perceiving all



Figure 6: SIMONA Research Simulator outside view (left) and inside view (right, with both outside visuals and hover display enabled at the same time).

system states in both visibility configurations, this section compares the time response of the developed model with data recorded during an experiment in the SRS.

The experiment took place in the SRS without motion. A non-linear six-degrees-of-freedom Bo105 model was used¹⁴. Two helicopter pilots (100-120 flight hours) participated voluntarily and without compensation. The task closely resembles the hover task described in the Aeronautical Design Standard 33E-PRF (ADS-33)¹⁵. The goal of the task is to approach a predefined hover target point at a height of 2 m and hover in place for 30 s. The full task description given to the pilot is:

Approach the hover target point with the initial forward speed of the helicopter at the beginning of the run. At a distance you deem appropriate, initiate a deceleration manoeuvre to smoothly and precisely come to a stop at the hover point. After reaching the hover point, maintain a stabilised hover, minimising deviations from the hover target point, for thirty seconds. Please avoid accomplishing most of the deceleration manoeuvre well before the hover point and then creeping up to the final hover position.

The proposed course set-up of ADS-33 is implemented in the outside visuals of the SRS. Desired and adequate hover position areas are denoted by the hover-board directly in front of the hover target, and by cones on the tarmac, placed to the right and in the front of the hover target point. The task was conducted either with good visibility and deactivated hover display, or with zero visibility and activated hover display. Figure 5 shows the employed hover display and basic instrument, Figure 6 depicts the SRS in both conditions at the same time.

The task was modified slightly, compared to ADS-33. Instead of starting in a 45° rotated position

Table 3: Helicopter state perception during ADS-33 hover task.

	Outside View	Instrument Panel	Hover Display
q	Visual flow	Artificial horizon pitch speed	Acceleration cue longitudinal speed
θ	Target board pitch position	Artificial horizon pitch position	Acceleration cue longitudinal position
u	Visual flow, edge rate	Speed metre	Velocity cue longitudinal direction
x	Longitudinal cone position	-	Hover target longitudinal position
w	Visual flow, edge rate	Altitude rate metre	-
z	Board vertical indication	Altimeter	-
p	Visual flow	Artificial horizon bank speed	Acceleration cue lateral speed
ϕ	Horizon bank position	Artificial horizon bank position	Acceleration cue lateral direction
v	Visual flow, edge rate	-	Velocity cue lateral direction
y	Board lateral indicator	-	Hover target lateral Position
r	Visual flow	Compass rose rotational speed	Display edge rotational speed
ψ	Board/cone yaw position	Compass rose rotational position	Display edge rotational position

close to the hover target, the starting point was situated at a distance of approximately 100 m to the hover target, facing it head-on. The starting distances were quasi-randomised by drawing points out of a probability distribution with a mean of 100 m and a standard deviation of 10 m. The drawn starting positions were identical and kept in the same order for every experiment condition. The starting velocity was kept constant at $10 \frac{m}{s}$ for every experiment run.

During the experiment, it became clear that executing the task while only utilising the hover display and instrument panel (without outside visuals) was not possible within the constraints of the experiment, which limited the training time to less than ten minutes per experiment condition. Therefore, only data for the conditions with good outside visuals are used in this paper. The data serve as a tool to qualitatively compare the developed pilot model with the behaviour of human pilots. Possible reasons for the closed-loop instability while utilising the hover display are discussed in Section 6.

Figure 7 depicts the geodetic longitudinal position x_{geo} , velocity \dot{x}_{geo} and acceleration \ddot{x}_{geo} of the helicopter in relation to the hover goal ($x_{geo} = 0$ m) during deceleration manoeuvres piloted by the pilot model and by the invited pilots, both with and without a SAS. The target trajectory for the pilot model is a *constant deceleration τ -guide*¹⁰ with $\tau = 0.6$. Lockett¹⁶ found that this τ -value shows good correlation with decelerations flown by helicopter pilots.

The pilot model and the invited pilots seem to follow a similar strategy: reduce the velocity almost linearly in time, until smoothly transitioning to a zero-velocity state close to the target. Without a SAS, the invited pilots changed their control behaviour when in close proximity to the hover target point ($x \approx -10$ m), initiating a phase of somewhat constant velocity until reaching the hover point. This behaviour is apparent in the position-plot through the gap between the pilot model and the invited pilot

trajectories at around 15 seconds into the manoeuvre.

There seems to be a good qualitative match between the deceleration trajectories of the developed pilot model and of the invited pilots, despite the fact that the invited pilots flew a non-linear model, while the pilot model was applied to a linear model. As previously mentioned, this similarity only holds for good outside visuals. While switching to a hover display doesn't change the pilot model's behaviour at all — the same input parameters are used — there are clearly additional complications for the invited human pilots. In the next section, possible reasons for the increased task difficulty are discussed.

6. DISCUSSION

This section combines the results of the previous three sections to discuss reasons for hover-display-incurred instability (in Subsection 6.1) and design recommendations to counteract the negative effects (in Subsection 6.2).

6.1. Reasons for instability

All invited pilots were able to control the helicopter with good outside visuals. The reason for closed loop instability while using the hover display therefore lies in the effect of the differences between using outside visuals and using the hover display (combined with the primary instrument panel) to control the helicopter. The major differences are:

1. loss of peripheral visual information;
2. loss of flow field information;
3. new requirement to scan multiple displays (altitude only available on altimeter, far from hover display); and

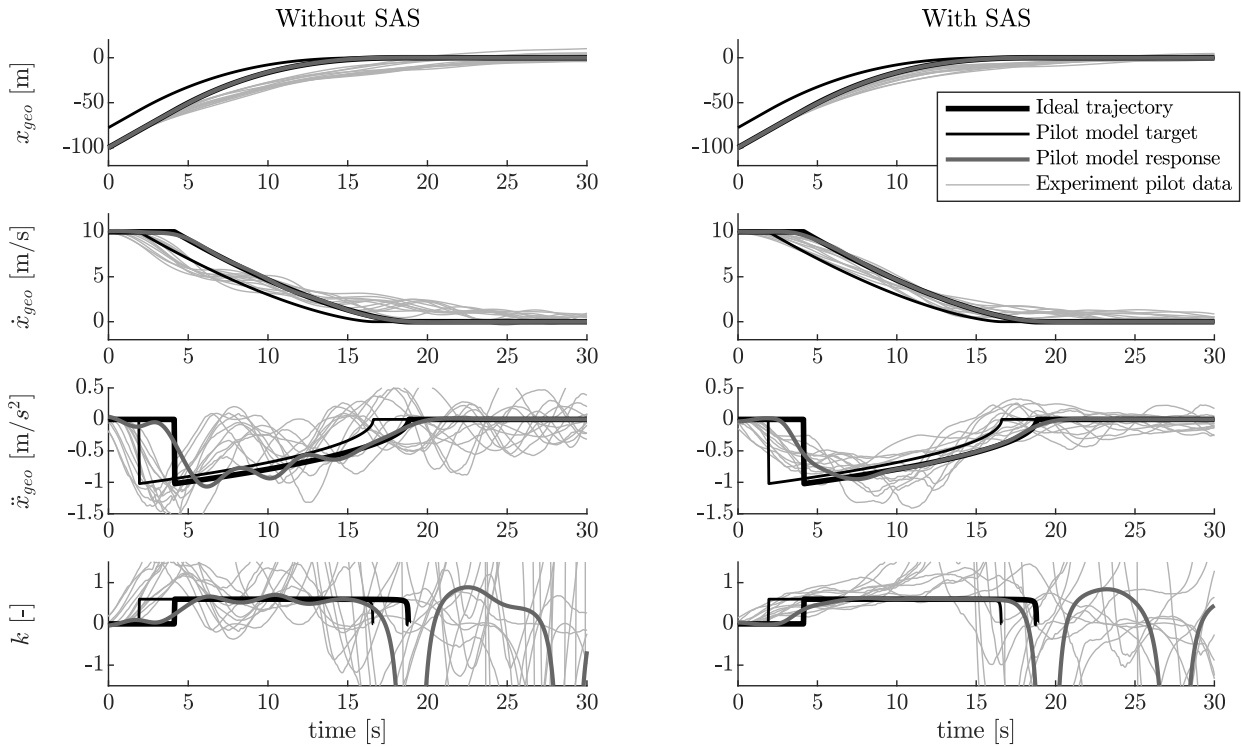


Figure 7: Approach-to-hover trajectories: ideal, pilot model target, pilot model response, and experiment pilot data.

4. new requirement to translate abstract top-down position and attitude information to existing mental model (or: new requirement to adapt mental model to new representation of flight state data).

Difference no. 1, as explained by Hosman and Stassen¹¹, leads to an increased perception time-delay. Similarly, as Yamaguchi et al.¹⁷ describe, the perception of an *illusory motion* helps performing a positioning task. Difference no. 2 eliminates the perception of an *illusory motion*, only abstract display information remains. This could lead to an increase in required processing time for the pilot to translate the perceived information to his mental model of the vehicle (difference no. 4). This is made harder by the physical distance between the displays the pilot has to integrate data from (difference no. 3). The heave control loop in particular might suffer from an increased time-delay, as the display to perceive altitude is located far away from the hover display. The pilot might be tempted to focus on the hover display and scan the altimeter less frequently, as the altimeter only supplies two of all the necessary flight data parameters.

Yamaguchi et al.¹⁷ elaborate on their idea of a mental model that is used to perform a control task. They imply that changing display arrangements

doesn't immediately make the controller adapt his or her mental model of the system. He or she rather has to adapt the information to fit his or her model. This supports the notion that with sufficient training, pilots would be able to adapt their mental model to fit the more abstract information presented by the hover display, enabling them to utilise the presented information better. In the current experiment, there was no sufficient time to perform this training step. The pilots immediately needed to interpret the abstract data to fit their internal mental model. This is expected to have incurred an additional time-delay, as explained before.

6.2. Hover display recommendations

To best support the pilot, a good hover display design should try to minimise the negative effect of the differences between using good outside visuals and using the hover display. Of the four discussed differences in the previous subsection, only difference no. 3 can be rectified within the constraints of a head-down hover display; placing an altitude tape close to the hover display in the cockpit would lessen the strain of having to scan multiple displays to acquire all necessary flight data information.

The other differences are inherent to head-down

hover displays — they can provide neither peripheral nor flow field information. The information is per definition displayed in an abstract, top-down manner, which requires pilots to change the way they translate the visual inputs to control outputs.

There might be ways of scaling hover displays such that they more closely resemble outside visual information. For example, the velocity and acceleration scaling factors could be tuned such that one degree of pitch- or roll-angle relates to a display cue that covers one degree of visual separation on the display, as seen from the pilot. On the other hand, this would imply a direct linear relation between attitude angle and horizontal acceleration, which holds true approximately, but not in all possible cases. It is questionable whether creating these similar scaling factors would help the pilot, or whether it would complicate the information integration even more.

7. CONCLUSION

This paper reinforced that head-down hover displays have inherent limitations; they are not well suited to be the only supplier of flight data for the pilot. For good outside visuals, the developed pilot models based on crossover-theory produce similar control strategies than human pilots during a simulator experiment. The models do not capture the added difficulties of using only a hover display and an instrument panel to control the helicopter.

The results of this paper suggest that the loss of peripheral and flow information and the added requirements on the pilot incurred by hover displays cause an additional time-delay greater than the time-delay stability margin of the pilot model and of the pilots who participated in the experiment. It is possible to counteract an additional time-delay by tuning the parameters of the control strategy. However, this additional tuning did not take place in this paper, because the invited pilots only had a very short training time of a few minutes per experiment condition. This limited their options of adjusting their control strategy to the hover display and instrument panel.

Hover displays without guidance cues do not work well as the sole source of flight data information. Future work will focus on augmented reality visualisations, implemented via HMDs or HUDs. These systems have shown the capability to replace the pilot's outside view and to introduce additional cues and support systems without severely limiting the pilot's ability to safely and freely[†] fly the aircraft.

[†]Freely implies neglecting the provided guidance cues and choosing a different action, caused by, e.g., unexpected events.

ACKNOWLEDGEMENTS

This study has been carried out in the context of the European Joint Doctorate NITROS (Network for Innovative Training on Rotorcraft Safety) project, whose main goal is to enhance rotorcraft safety by addressing critical aspects of their design.

This project has received funding from the European Union's Horizon 2020 research and innovation programme under the Marie Skłodowska-Curie grant agreement N° 721920.

REFERENCES

- [1] Minor, J., Morford, Z., and Harrington, W., "Sensor data/cueing continuum for rotorcraft degraded visual environment operations," *Proceedings Volume 10196, Degraded Environments: Sensing, Processing, and Display 2017, SPIE Defense + Security*, International Society for Optics and Photonics, Anaheim, California, United States of America, 2017.
- [2] Münsterer, T. R., Singer, B., Zimmermann, M., and Gestwa, M., "NIAG DVE flight test results of LiDAR based DVE support systems," *Proceedings Volume 10642, Degraded Environments: Sensing, Processing, and Display 2018, SPIE Defense + Security*, International Society for Optics and Photonics, Orlando, Florida, United States of America, 2018.
- [3] Stanton, N. A., Plant, K. L., Roberts, A. P., Allison, C. K., and Harvey, C., "The virtual landing pad: facilitating rotary-wing landing operations in degraded visual environments," *Cognition, Technology & Work*, Vol. 20, No. 2, may 2018, pp. 219–232.
- [4] Hess, R. A. and Gorder, P. J., "Design and evaluation of a cockpit display for hovering flight," *Journal of Guidance, Control, and Dynamics*, Vol. 13, No. 3, may 1990, pp. 450–457.
- [5] Eshow, M. M. and Schroeder, J. A., "Improvements in hover display dynamics for a combat helicopter," *Piloting Vertical Flight Aircraft: A Conference on Flying Qualities and Human Factors*; p 235-250, jul 1993.
- [6] Szoboszlay, Z. P., McKinley, R. A., Braddom, L. S. R., Harrington, W. W., Burns, H. N., and Savage, J. C., "Landing an H-60 helicopter in Brownout Conditions Using 3D-LZ Displays," *Proceedings of the American Helicopter Society 66th Forum*, Phoenix, Arizona, United States of America, 2010.
- [7] North Atlantic Treaty Organization Advisory Group for Aerospace Research and Development, "AGARD Report 594: V/STOL Displays for

Approach and Landing," Tech. rep., London, 1972.

- [8] Padfield, G. D., *Helicopter Flight Dynamics: The Theory and Application of Flying Qualities and Simulation Modeling*, American Institute of Aeronautics and Astronautics, 2nd ed., 2007.
- [9] McRuer, D. T. and Jex, H. R., "A Review of Quasi-Linear Pilot Models," *IEEE Transactions on Human Factors in Electronics*, Vol. HFE-8, No. 3, 1967, pp. 231–249.
- [10] Padfield, G. D., "The Tau of Flight Control," *The Aeronautical Journal*, Vol. 115, No. 1171, 2011, pp. 521–556.
- [11] Hosman, R. J. A. W. and Stassen, H. G., "Pilot's Perception and Control of Aircraft Motions," *IFAC Proceedings Volumes*, Vol. 31, No. 26, sep 1998, pp. 311–316.
- [12] Drop, F. M., *Control-Theoretic Models of Feedforward in Manual Control*, Ph.D. thesis, Delft University of Technology, 2016.
- [13] Barendswaard, S., Pool, D. M., Van Paassen, M. M., and Mulder, M., "Dual-Axis Manual Control: Performance Degradation, Axis Asymmetry, Crossfeed, and Intermittency," *IEEE Transactions on Human-Machine Systems*, Vol. 49, No. 2, apr 2019, pp. 113–125.
- [14] Miletović, I., Pool, D. M., Stroosma, O., Pavel, M. D., Wentink, M., and Mulder, M., "The Use of Pilot Ratings in Rotorcraft Flight Simulation Fidelity Assessment," *Proceedings of the American Helicopter Society 73rd Forum*, Fort Worth, Texas, United States of America, 2017.
- [15] Anonymous, "Aeronautical Design Standard - 33E PRF, Performance Specification, Handling Qualities Requirements for Military Rotorcraft," US Army AMCOM, Redstone, Alabama, United States of America, 2000.
- [16] Lockett, H. A., *the Role of Tau-Guidance During Decelerative Helicopter Approaches*, Ph.D. thesis, University of Liverpool, 2010.
- [17] Yamaguchi, M. and Proctor, W. R., "Compatibility of motion information in two aircraft attitude displays for a tracking task," *The American Journal of Psychology*, Vol. 123, No. 1, 2010, pp. 81.

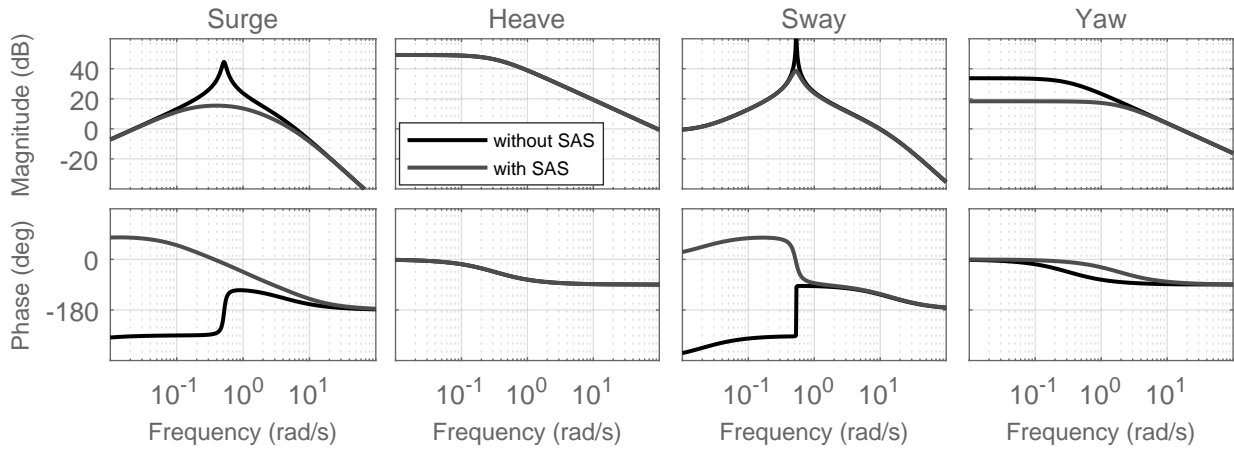


Figure 8: Bode plots of the inner loop controlled element transfer function $Y_{c,inner}$ for surge, heave, sway, and yaw.

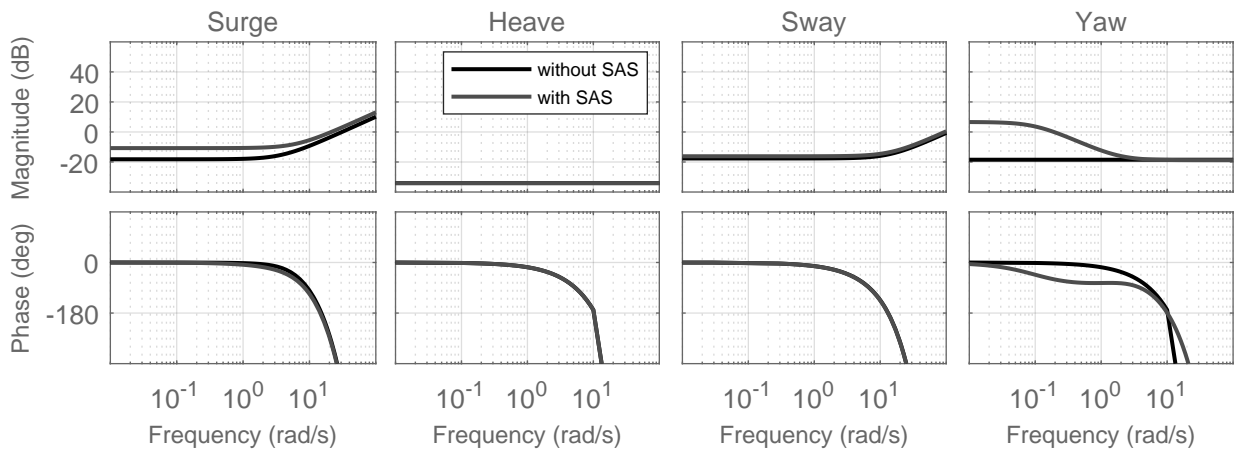


Figure 9: Bode plots of the inner loop pilot model transfer function $Y_{p,inner}$ for surge, heave, sway, and yaw.

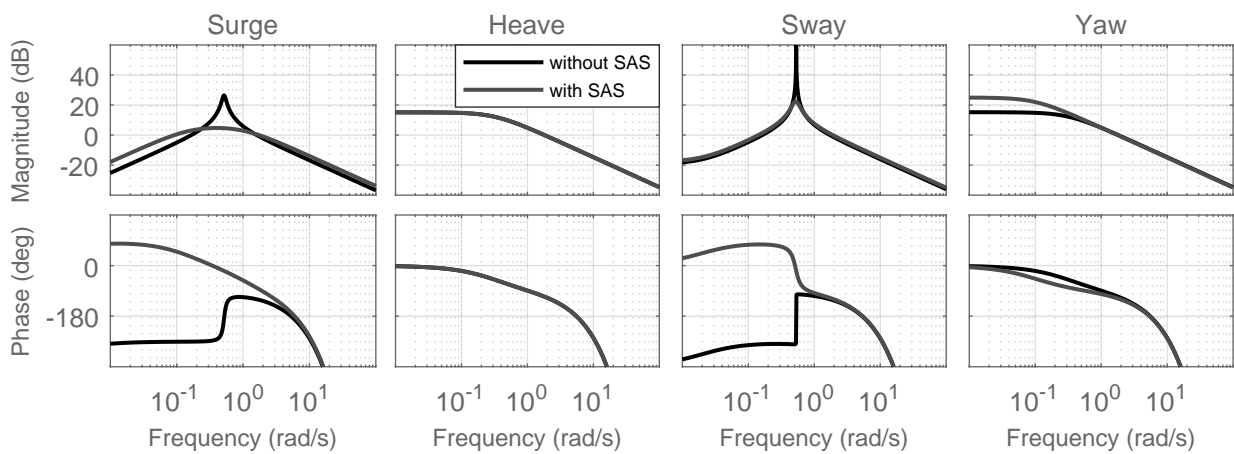


Figure 10: Bode plots of the inner loop open loop transfer function $Y_{OL,inner}$ for surge, heave, sway, and yaw.

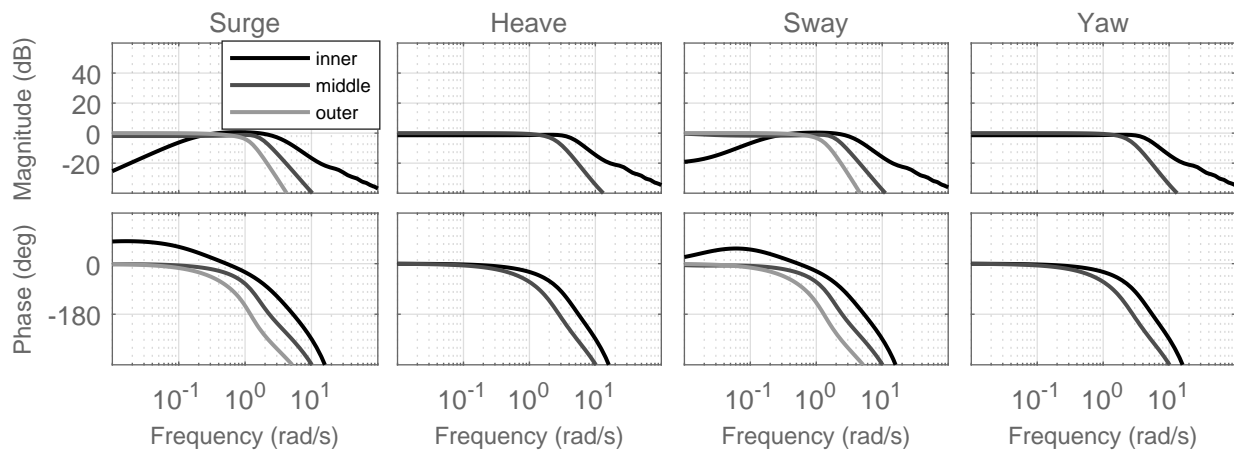


Figure 11: Bode plots of the inner, middle, and outer loop closed loop transfer functions Y_{CL} for surge, heave, sway, and yaw without SAS.

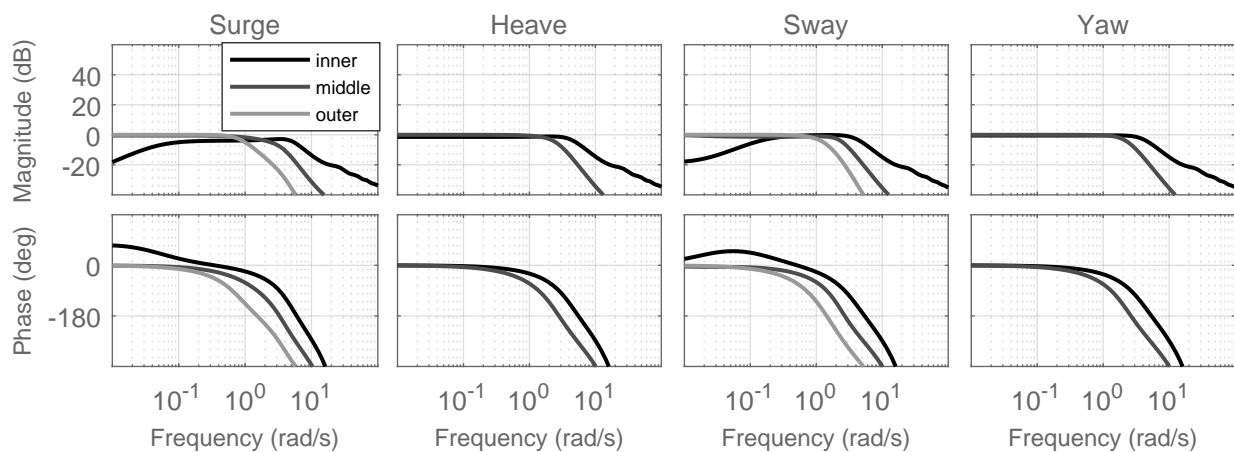


Figure 12: Bode plots of the inner, middle, and outer loop closed loop transfer functions Y_{CL} for surge, heave, sway, and yaw with SAS.